Preparation and Characterization of Poly(D,L-lactic-*co*-glycolic acid) Nanoparticles Containing 3-(Benzoxazol-2-yl)-7-(*N*,*N*-diethyl amino)chromen-2-one

Anderson J. Gomes,[1] Rosana Maria Nascimento Assunção,[2] Guimes Rodrigues Filho,[2] Enilza M. Espreafico,[3] Antonio Eduardo da Hora Machado[1]

[1]*Laboratório de Fotoquímica/Grupo de Fotoquímica e Química da Madeira (GFQM), Instituto de Química, Universidade Federal de Uberlândia, P.O. Box 593, 38400-902 Uberlândia, Minas Gerais (MG), Brazil*
[2]*Laboratório de Reciclagem de Polímeros, Instituto de Química, Universidade Federal de Uberlândia, P.O. Box 593, 38400-902 Uberlândia, MG, Brazil*
[3]*Laboratório de Biologia Celular e Molecular e Bioagentes Patogênicos, Faculdade de Medicina de Ribeirão Preto da Universidade de São Paulo (FMRP/USP), São Paulo, Brazil*

Received 11 December 2005; accepted 30 November 2006
DOI 10.1002/app.26204
Published online 6 April 2007 in Wiley InterScience (www.interscience.wiley.com).

ABSTRACT: Nanoparticles (NPs) of poly(D,L-lactic-*co*-glycolic acid) containing the compound 3-(benzoxazol-2-yl)-7-(*N*,*N*-diethyl amino)chromen-2-one (C2) were prepared by the solvent-evaporation technique with a mean loading efficiency of 74.0 ± 3.0%. Size distribution studies, done with dynamic light scattering and scanning electron microscopy, revealed that these particles were spherical in shape, with a mean diameter of 253 nm, a low polydispersity, and a tendency toward aggregation; the last was confirmed by the low ζ potential. A low release profile was observed for C2 when the NPs were dispersed in Hank's buffer (pH = 7.4); this was related to the low porosity of the NPs and the extremely low diffusivity of C2 in water. Differential scanning calorimetry data presented a glass-transition temperature depression caused by an increase in the NP molecular mobility after the incorporation of C2. Spectroscopic and photophysical data exploring the capabilities of C2 as a fluorescent probe suggested a high microviscosity for the environment in which the probe was allocated, which was most likely due to strong polar interactions involving ester groups from the polymer and the diethylamino moiety from C2. The cellular toxicity and uptake of C2 and NP–C2 systems were evaluated with B16-F10 murine cells, which showed that C2 (in solution or encapsulated) was nontoxic and able to be located inside the neoplasic cells. Besides, the encapsulation method was capable of maintaining the drug's properties and improved the drug delivery to the target cell. © 2007 Wiley Periodicals, Inc. J Appl Polym Sci 105: 964–972, 2007

Key words: biocompatibility; differential scanning calorimetry (DSC); drug delivery systems; dynamic light scattering; fluorescence; FTIR; nanoparticles; photophysics

INTRODUCTION

The study of nanoparticles (NPs) prepared from a polyester, poly(D,L-lactic-*co*-glycolic acid) (PLGA), has attracted increasing interest because of their biodegradability, biocompatibility, and capacity to efficiently accommodate and transport drugs.[1–3] The *in vivo* degradation of such materials occurs by the hydrolysis of the ester linkages under acid-, base-, and enzymatically catalyzed processes, lactic ($C_3H_6O_3$) and glycolic ($C_2H_4O_3$) acids being degradation intermediates,[4–8] resulting subsequently in CO_2 and H_2O via the Krebs cycle.[9] In particular, NPs could offer a number of advantages with respect to other delivery systems because (1) they maintain unaltered their physicochemical characteristics for long periods, allowing long-term storage; (2) according to their composition, they can be administered in different ways (orally, intramuscularly, or subcutaneously); and (3) they are suitable for industrial production.[10,11]

In an attempt to enhance the therapeutic efficacy of NP-encapsulated therapeutic agents, the understanding of the mechanisms of their intracellular and tissue distribution is fundamental.[8]

Coumarin is a family of compounds extensively studied because of their practical applications, which include biological and chemical sensors, fluorescent probes, dye lasers, optical brighteners, and sensitizers in phototherapy.[12–21] In particular, the use of fluores-

Correspondence to: A. de Jesus Gomes (anderson@iqufu.ufu.br) or A. E. da Hora Machado (aeduardo@ufu.br).

Contract grant sponsor: Conselho Nacional de Desenvolvimento Científico e Tecnológico (through a postdoctoral grant to A.J.G.); contract grant number: 303911/2003-4.
Contract grant sponsor: Conselho Nacional de Desenvolvimento Científico e Tecnológico (to A.E.H.M.).
Contract grant sponsor: Fundação de Amparo à Pesquisa do Estado de Minas Gerais (to A.E.H.M.).

cent probes allows us to access structural and physicochemical parameters related to the structure of organized microenvironments,[22] such as micelles, vesicles, microparticles, and NPs.

Despite other classes of organic compounds used as fluorescent probes,[23,24] the 7-aminocoumarins have attracted attention because of their unusual solvatochromic and photophysical characteristics,[12,15,25–29] which tend to make them advantageous for this aim.

Considerable attention has been given in our research group to the study of the luminescent properties of the compound 3-(benzoxazol-2-yl)-7-(*N*,*N*-diethylamino)chromen-2-one (C2; Scheme 1), which has demonstrated potential as a fluorescent probe.[12,15] Gao et al.[30] estimated $E_T(30)$, polarity parameter defined as the molar transition energy corresponding to the longest-wavelength, values in the range between 52.7 and 57.7 kcal/mol for micelle environments formed by sodium dodecyl sulfate in water, using three 7-amino-substituted hetocoumarins. Using C2, under similar conditions, we estimated an $E_T(30)$ value of 55.7 kcal/mol,[15] whereas in a buffered medium (a phosphate buffered saline, PBS) the estimated value was 61.3 kcal/mol,[12] showing the good sensitivity of this probe.

In this work, PLGA NPs were characterized with different techniques. The effect of C2 encapsulation on their physical properties (e.g., surface charge and particle size) and on NP cellular uptake was evaluated. Also, on the basis of the capability of C2 as a chemical sensor, some physical characteristics of the NPs could be evaluated by differential scanning calorimetry (DSC) and spectroscopic techniques.

EXPERIMENTAL

General

Compound C2 was synthesized by Oliveira-Campos et al.[31] PLGA (50 : 50, weight-average molecular weight = 17 kDa) was purchased from Sigma Chemical, Inc. (St. Louis, MO). Poly(vinyl alcohol) (PVA; 13–23 kDa, 87–89% hydrolyzed) was supplied by Aldrich Chemical Co. (Milwaukee, WI). Dichloromethane and all other chemicals were analytical-grade, were supplied by Vetec (Rio de Janeiro, Brazil), and were used without further purification.

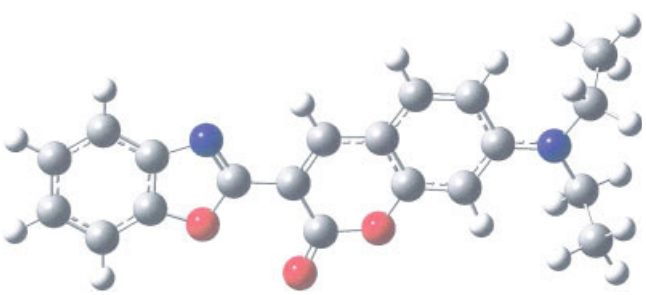

Scheme 1 Representation of compound C2. [Color figure can be viewed in the online issue, which is available at www.interscience.wiley.com.]

Preparation and characterization of the NPs

The methodology for the preparation of NPs containing C2 (10 μM) was based on a previous work.[32] The particle size and morphology were assessed by photon correlation spectrometry (Zetasizer 3000, Malvern Instrument, Worcestershire, UK) as well as scanning electron microscopy (SEM; ESEM 2020, Philips, Eindhoven, The Netherlands). The ζ potential of the NPs (1.0 mg/mL) in 0.1 m*M* Hank's buffer (pH 7.4) was determined with a ZetaPlus (Malvern Instrument).

The amount of C2 incorporated into the NP was estimated spectrophotometrically (UV-250 1 PC, Shimadzu, Kyoto, Japan) by a direct method that consisted of the dissolution of aliquots containing 10 mg of C2-loaded NPs (NP–C2) in methylene chloride and the assessment of the drug concentration by means of its absorbance at 450 nm. The drug incorporation efficiency was expressed as the percentage of incorporated C2 with respect to the total amount of drug added. The loading efficiency [L (%)] was calculated as follows:

$$L\ (\%) = (L_A/L_T) \times 100 \quad (1)$$

where L_A is the amount of C2 in the NP and L_T is the total amount of the drug added.

The residual amount of PVA associated with the NPs was determined by a colorimetric method proposed by Sahoo et al.[33]

The physical state of the aminocoumarin inside the NPs was characterized by thermal analysis (DSC SP, Rheometric Scientific, New Jersey). The samples were sealed in aluminum pans with lids and purged with ultrapure dry nitrogen at a flow rate of 20 mL/min. The temperature ramp was set at 10°C/min, and the heat flow was recorded in the range between 30 and 100°C. Indium was used as a standard to calibrate the temperature and energy scales of the DSC instrument.

C2 release kinetics

The C2 release kinetics were determined in Hank's buffer at 37°C. The released aminocoumarin was quantified by the monitoring of its fluorescence (F4500, Hitachi, Tokyo, Japan) in the supernatant after centrifugation. For this, after centrifugation, the supernatant was evaporated at 25°C. After that, it was dissolved in an aliquot of 2 mL of dichloromethane, the fluorescence spectrum being measured in the range between 450 and 700 nm (excitation wavelength = 442 nm). The amount of released material could be estimated with a standard curve. All measurements were done in triplicate.

Spectrophotometric and fluorescence assays

A PerkinElmer (Norfolk, CT) Spectrum 1000 Fourier transform infrared (FTIR) spectrophotometer was used to record the IR spectra of the polymers, NPs, and coumarin derivative. The samples were prepared by the mixing of the materials with KBr in a proportion of 1 : 100 (w/w). For all spectra, 32 scans were accumulated with a 4-cm^{-1} resolution.

The ultraviolet–visible absorption attributed to the coumarin incorporated into the NPs was determined by the deconvolution of the NP–C2 absorption spectrum with a program based on the self-modeling factor analysis method.[34]

The fluorescence quantum yield (Φ_F) values of C2 were estimated from the corrected fluorescence spectra with the secondary standard method.[35] The fluorescence standard was 9,10-diphenylanthracene in cyclohexane ($\Phi_F = 0.90$ at 293 K). The solutions were prepared in such a way as to keep the absorbance below 0.100 at the excitation wavelength to avoid light reabsorption effects.

C2 and NP–C2 cytotoxicity and NP uptake

To evaluate the C2 and NP–C2 cytotoxicity, a B16-F0 cell line was seeded at 5000 cells/well in 96-well plates. The cells were kept in 100 μL of fresh HAM-F10 media (supplemented by 10% fetal calf serum and antibiotics at 100 U/mL) for 24 h to allow cell adhesion and environmental adaptation. Subsequently, these cells were treated with an additional 100 μL of HAM-F10 containing different concentrations of C2 and NP (0–1 mg/mL) for 24 h. After this interval, the medium was removed, and the wells were washed three times with PBS media alone before the addition of 50 μL of a 1 mg/mL yellow tetrazolium dye [3-(4,5-dimethylthiazolyl-2)-2,5-diphenyltetrazolium bromide (MTT)]. After that, the plates were returned to the incubator for a period of 4 h. The residual MTT solutions were removed from wells, and then 200 μL of dimethyl sulfoxide was added to each well. The plates were stored at room temperature in a dark place for more 30 min before being read at 570 nm with an XFluor Plate Reader (Tecan US, Inc., Durham, NC). The cell viability percentage was calculated with respect to control cells incubated without C2 and NP. All experiments were performed in triplicate.[36]

The NP uptake was determined by the incubation of B16-F10 cells with NP–C2 for 2 h under the same conditions employed for the dark toxicity assay. After incubation, the cells were observed by phase-contrast and fluorescence microscopy [the fluorescence label was observed with a Nikon Elipse (Tokyo, Japan) TS 100 microscope equipped with 1.4 numerical aperture 63× and 100× objectives (Zeiss, Oberkochen, Germany) and recorded with a Photometrics cooled charge-coupled device camera].

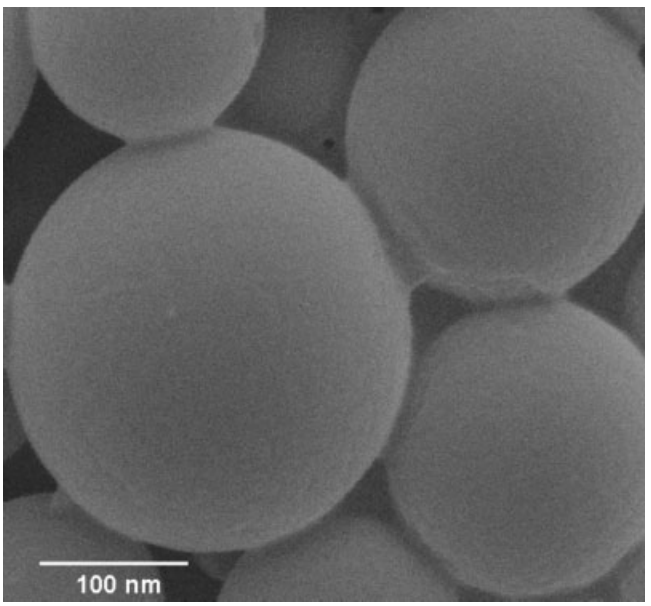

Figure 1 Surface morphology of coumarin-derivative-loaded NPs prepared by the solvent-evaporation method. The original magnification was 35,000× by SEM. The scale bar is equal to 100 nm.

Quantum mechanical calculations

Quantum mechanical calculations were performed for the isolated molecule in the ground state with a density functional theory method (B3LYP) and a doubly polarized basis function [6-31G(d,p)] from the Gaussian 03W suite of programs.[37] The Berny analytical gradient was used in the optimization. From the optimized structure, the electron density map for the molecule was built.

RESULTS AND DISCUSSION

Preparation of the PLGA NPs and evaluation of their morphology

Figure 1 shows a representative micrograph of NP–C2 magnified at 35,000×. In all preparations reported in this article, the NPs were spherical in shape, displaying a smooth surface. No meaningful difference was found between C2-containing PLGA NPs and the empty nanoparticle (ENP) used as a control, except for size variations.

Efficiency of the drug entrapment and PVA assay

The C2 incorporation was 74.0 ± 3.0% (i.e., 3). In general, high encapsulation rates of hydrophobic drugs are relatively easy to reach with hydrophobic polymers such as PLGA because of their limited drug loss

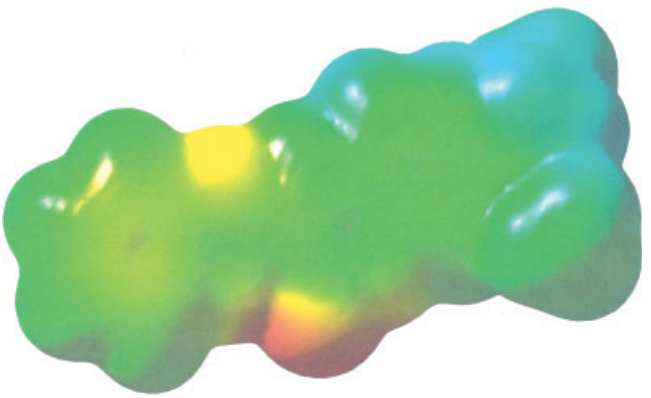

Figure 2 Electron density map of C2 calculated with a method from density functional theory. The regions in red present high electronic density, whereas the regions in blue reflect a strong concentration of positive charge density. [Color figure can be viewed in the online issue, which is available at www.interscience.wiley.com.]

to the aqueous phase. Additionally, the encapsulation efficiency reached for this aminocoumarin can be attributed to the use of 3.0% PVA in the formulation, unlike what was proposed by Schlicher et al.[38] According to Kompella et al.,[39] PVA stabilizes oil-in-water emulsion globules, thereby reducing a drug's diffusion to the aqueous medium. In fact, it has been shown that when PVA is used as a surface stabilizer for PLGA NPs prepared by a double-emulsion and solvent-evaporation method, a fraction of PVA forms a stable network on the polymer surface that cannot be removed during a washing procedure. It is important to point out that PLGA is negatively charged because of the presence of carboxylic groups. Therefore, the fraction of residual PVA on particle surfaces should shield the surface charge as well as the other polymers able to coat PLGA particles.[40] The estimated percentage of residual PVA is in the range of 1.2–3.1% (w/w) for these formulations.

Particle size and surface charge (ζ potential)

The solvent-evaporation method produces particles with a mean diameter around 253 nm (±42 nm) when loaded with the aminocoumarin, which is slightly higher than the size of the ENPs, which is around 207 nm (±38 nm).[32] For all formulations analyzed by dynamic light scattering, a unimodal size distribution was observed, with a polydispersity index lower than 0.5. The particle size is an important property that affects the intracellular uptake of NPs, with smaller particles in general having higher uptake rates. Thus, the particle size could also affect the efficacy of NP-encapsulated therapeutic agents.[8]

The colloidal stability was analyzed by the measurement of the ζ potential of the NPs. In this study, the coumarin-free NPs are negatively charged, presenting a ζ potential of −1.3 mV at pH 7.4, whereas NP–C2 presents a slightly positive ζ potential (+0.5 mV), suggesting that C2 does not show a trend to suffer aggregation inside the NPs. The positive ζ potential should be due to polar interactions between C2 and carboxylic groups present at the surface of PLGA particles.

The analysis of a C2 electron density map (Fig. 2) suggests that this interaction involves specifically the diethylamino moiety, which possesses a strong concentration of positive charge density (blue color). It is known that C2 is a typical electron-donor/acceptor molecule because of intramolecular charge transfer.[12]

It is currently accepted that suspensions with ζ potentials lower than −30 mV or greater than +30 mV are not likely to aggregate.[40] Under most conditions, the higher the absolute value is of the ζ potential of the NPs, the larger the charge is on their surface, leading to stronger repulsive interactions between the dispersed NPs and resulting in higher stability and a more uniform size.[2,7,40]

FTIR

Figure 3 presents the FTIR spectra of PVA, ENPs, and NP–C2. As PLGA is the main component of the NPs, the FTIR spectrum of ENPs must be very similar to that obtained for this compound. Thus, the typical FTIR bands of PLGA (two medium intensity signals at 3650 and 3514 cm^{-1} attributed to O—H bond stretching, an intense and bifurcated signal at 3004 and 2954 cm^{-1} related to C—H stretching, an intense signal at 1760 cm^{-1} due to the C=O stretching from ester, and a set of signals between 1456 and 1380 cm^{-1} corresponding to C—H bending and at 1130 and 1090 cm^{-1} related to C—O stretching) are essentially the same as those observed in the ENP FTIR spectrum.

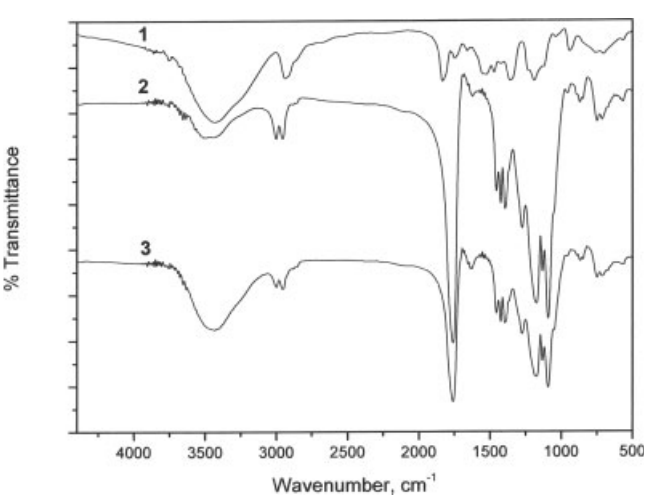

Figure 3 Superposition of FTIR spectra of (1) PVA, (2) ENPs, and (3) NP–C2.

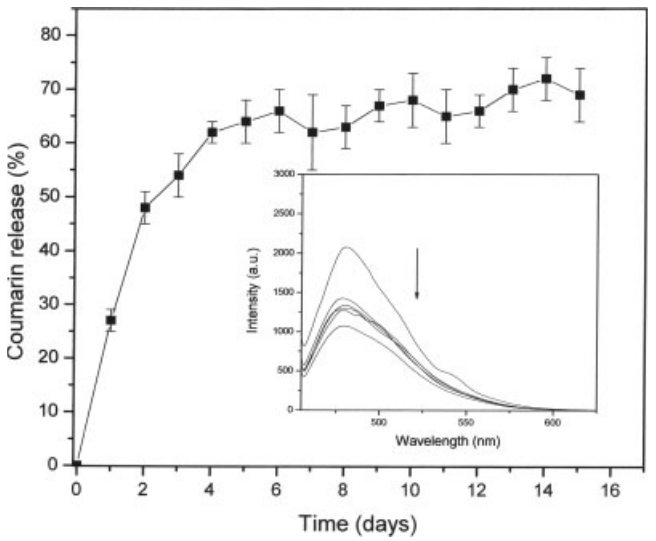

Figure 4 Cumulative release profile of coumarin from PLGA NPs into Hank's buffer medium (pH 7.4) in a period of 15 days.

On the other hand, as residues of PVA remain in the composition of the NPs after preparation and even after several washes,[2,41] the bands related to PVA are superimposed to the FTIR spectrum of ENPs.

The presence of small amounts of PVA in the formulation is desirable because it may be used to modulate the physical and cellular uptake properties of NPs. Panyam and Labhasetwar[8] suggested that the remaining PVA content associated with the NP surface affects positively the capability of cellular uptake, in comparison with particles with a lower amount of associated PVA.

On the other hand, because of the extremely small concentration of incorporated C2, the FTIR spectrum of the NPs loaded with C2 did not present important changes when compared with the ENP spectrum.

In vitro drug release

The release of C2 from PLGA NPs presents a biphasic pattern (Fig. 4). The day-to-day release was evaluated to obtain quantitative information on the C2 release profile in a disperse system in a period of 15 days. This was done in Hank's buffer. The burst effect in the initial phase of the release might be attributed to nonentrapped coumarin molecules adsorbed to the surface of the NPs or molecules able to be released through pores and channels that formed during its preparation.

The slow release of the encapsulated C2 should be due to the low porosity of the NPs, which is influenced by the nature of the formulation. This fact can be explained by the degradation of the PLGA polymer, which results in a sustained release of C2 to the bulk. Similar results were obtained with a benzopsoralen incorporated into microparticles and NPs,[42,43] suggesting that the low porosity, observed by SEM data, is a characteristic of the mode by which the PLGA NPs are prepared because the studied benzopsoralen presents a similar hydrophilic character.

DSC

This technique is frequently used to analyze the physical state of drugs encapsulated in polymeric NPs.[44] This analysis was performed to evaluate a possible interaction between the drug and the polymer. The first DSC thermograms (Fig. 5) for the empty and C2-containing NPs show a single endothermic peak close to the glass-transition temperature (T_g). A comparison with the calorimetric profile of the polymer suggests that this endotherm is related to the kinetic overshoot, which is superimposed to the polymer T_g.[45] This can be observed in a second scan of the DSC thermogram, which shows a decrease in the endothermic peak close to T_g (Fig. 5, inset). NP–C2 showed similar behavior.

The decrease in the T_g values for the ENP and NP containing C2 (NP–C2) in two sequential scans (in the first scan, $T_{g(\mathrm{ENP})} = 45.9^{\circ}\mathrm{C}$ and $T_{g(\mathrm{NP-C2})} = 41.4^{\circ}\mathrm{C}$, whereas in the second scan, $T_{g(\mathrm{ENP})} = 42.3^{\circ}\mathrm{C}$ and $T_{g(\mathrm{NP-C2})} = 39.9^{\circ}\mathrm{C}$) suggests the occurrence of an interaction between the polymer (PLGA) and C2. The incorporation of C2 increases the NP mobility because the polymer requires less energy to present collective movement of the chain segments, which results in the observed T_g depression.

The increase in the NP mobility due to the incorporation of C2 is followed by a reduction in the C2 mobility due to the highly viscous microenvironment in which it is allocated into the NPs, as verified by spectroscopic and photophysical data.

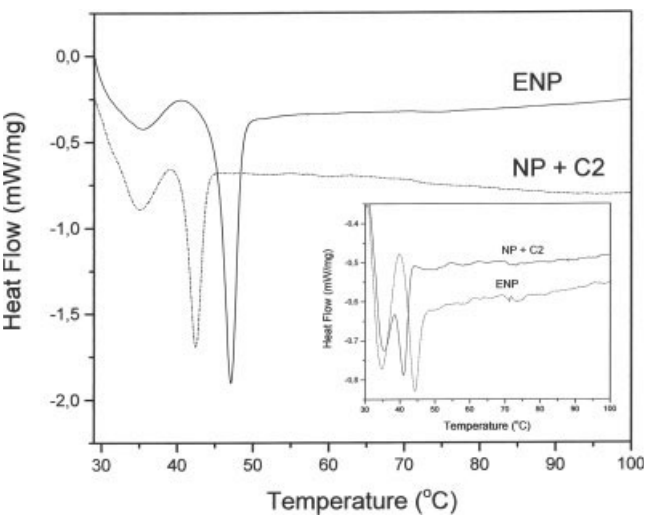

Figure 5 DSC thermograms of (- - -) empty PLGA NPs and (—) PLGA NPs containing coumarin. Pure PLGA was used as a control. The inset shows the second scan.

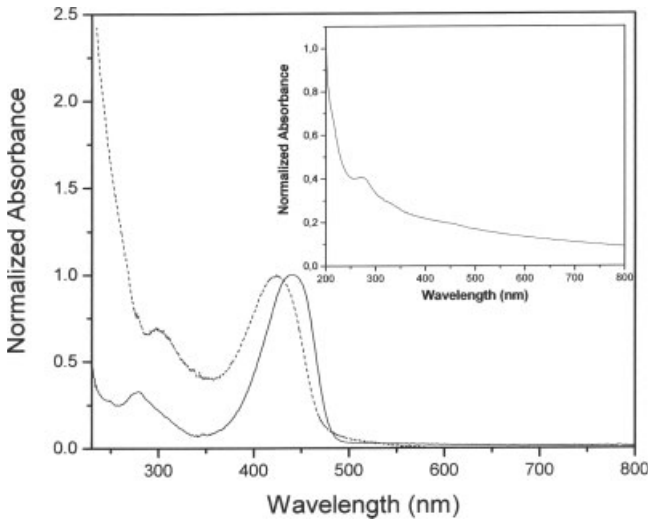

Figure 6 (—) Normalized absorption spectrum of coumarin in dichloromethane and (- - -) deconvoluted spectrum of coumarin. The inset shows PLGA NPs with coumarin in water.

Spectrophotometric and fluorescence assays

The long wavelength absorption of C2, attributed to an $S_0 \rightarrow S_1$ transition,[12] is characterized by an intense, broad, and nonstructured band sensitive to the solvent polarity, which is typical of $^1(\pi,\pi^*)$ transitions.[46,47] It possesses systematically high values of molar absorptivity between 40,000 and 54,000 L mol^{-1} cm^{-1}, which are also observed for analogue compounds.[12–15,19,20]

Seixas de Melo et al.,[48] studying the photophysics of coumarins, concluded that, for this class of compounds, the S_1 state is typically $^1(n,\pi^*)$ and that the energy gap between the S_1 and S_2 states is very close. In view of this, substitutions or changes in the solvent polarity may reduce the energy gap between these states, promoting the mixing or even the inversion. This explains the spectroscopic behavior of C2, which suggests that S_1 is a π,π^* state. This has been attributed to the combination of the electronic effects caused by the diethylamino and benzoxazole groups on the coumarin ring.[12]

The absorption spectrum of the NP–C2 in solution is characterized by an overlap of absorption bands in the UV, with considerable light scattering below 300 nm due to the NPs suspended in water. Using a deconvolution technique described elsewhere,[34] we can show that the spectrum of NP–C2 is a linear combination of only two spectra (Fig. 6). An inspection of the data indicated that the experimental and calculated spectra were perfectly superimposable,[34] with the sum of squares of the differences never exceeding 2.6×10^{-5}.

The C2 absorption spectrum in methylene chloride shows the long wavelength absorption band with a maximum at 439 nm, whereas when it is loaded into the NPs, this value is hypsochromically shifted to 430 nm (Fig. 6). This spectral shift confirms the occurrence of favorable polymer–C2 interactions in the microenvironments formed by the NPs, as suggested by the analysis of DSC and ζ-potential data, promoting the relaxation of the ground state and consequently an increase in the energy gap between this and the Franck–Condon state.

The small energy gap between the low-lying adjacent excited states of C2 plays an important role in the behavior of the excited state and consequently in the solvatochromic characteristics of this compound.[12] Despite the sensitivity of this compound to changes in the solvent polarity, the mixing of states tends to reduce the spectral shift of the absorption maximum corresponding to the $S_0 \rightarrow S_1$ transition. This indicates that the use of a correlation between the transition frequency (or wave number) of C2 and some empirical solvent polarity scale for probing a given system may result in less reliable data. On the other hand, the change in Φ_F as the solvent polarity varies is very expressive.[12] It is well established that Φ_F for 7-aminocoumarins is usually high, in some cases even close to unity.[49–51] The correlation between Φ_F and the $E_T(30)$ empirical solvatochromic scale[52] has given a useful and safe correlation for this aim.[12,15]

Figure 7 presents the normalized fluorescence spectra of C2 in dichloromethane and incorporated into the NPs. These fluorescence spectra are very similar in shape but present an emission maximum at 482 nm in dichloromethane and a redshifted value, with a peak around 487 nm, for NP–C2, suggesting that the interactions between C2 and the NPs result in good stabilization of the excited state, with its consequent relaxation. This is confirmed by the Stokes shift, which is

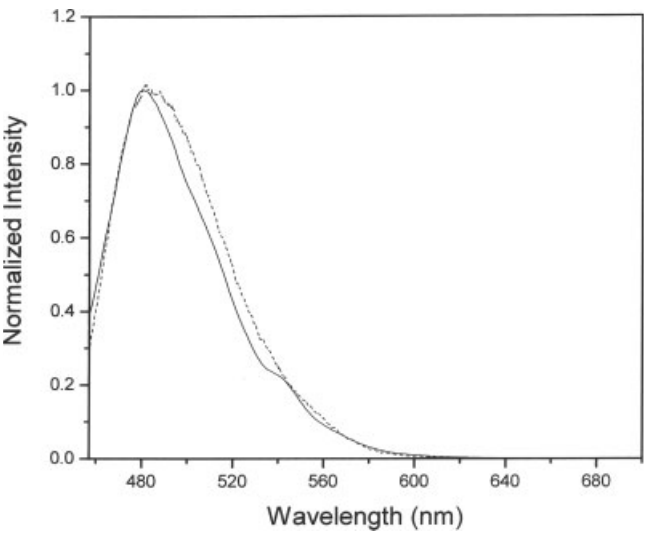

Figure 7 Normalized fluorescence spectra of (—) C2 in dichloromethane and (- - -) PLGA NPs.

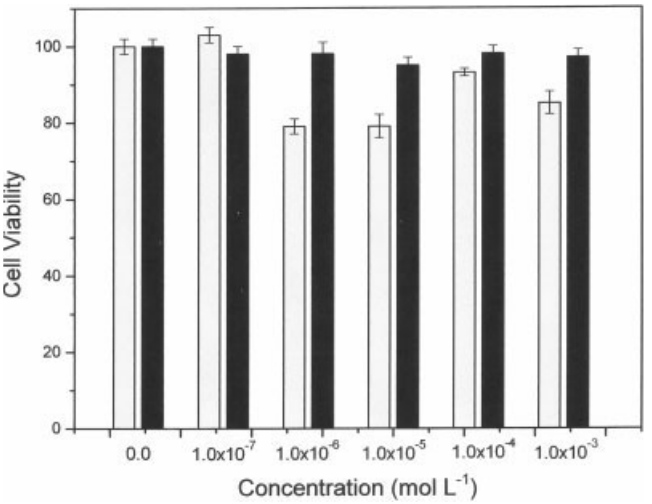

Figure 8 Cell viability quantified by an MTT assay: (□) C2 and (■) NP–C2. B16-F10 cells were incubated with different coumarin concentrations in Hank's medium.

higher for NP–C2 than for C2 in dichloromethane. As S_1 of C2 is a more polar state than S_0,[12] we can conclude that these interactions involve polar groups from NPs.

The shape of the observed emission spectra for NP–C2 and C2 in dichloromethane seems to be characteristic of the S_2 [intramolecular charge transfer (TICT)] state, also suggesting the occurrence of polar solute–solvent interactions performed by these two different media, capable of shifting the dynamic equilibrium between the S_1 [locally excited (LE)] and S_2(TICT) states toward the S_2(TICT) state.[12]

The comparison of the value of Φ_F (0.79) for NP–C2, slightly lower than that in dichloromethane ($\Phi_F = 0.86$), also shows that C2 performs more favorable polar interactions inside the NPs than with dichloromethane. It is known that specific intermolecular polar interactions involving the diethylamino group of electronically excited C2 implies an increase in the vibronic coupling, reducing Φ_F and consequently increasing the rate of internal conversion.[12] This can, under extreme conditions (e.g., intermolecular hydrogen bonding), lead to the formation of a hydrogen-bonded state (HICT).[12,53] Thus, it is plausible to consider that the decrease in the value of Φ_F should be related to polar intermolecular interactions inside the NPs, involving preferentially the ester groups from the NPs and the diethylamino moiety from C2.

The light scattering induced by the NPs in a suspension does not affect significantly the fluorescence measurements because the emission spectra were obtained with sufficiently diluted solutions and suspensions with the aim of avoiding internal filter effects.[35] Besides, the excitation wavelength (442 nm) is sufficiently shifted from the range at which strong light scattering is observed.

The $E_T(30)$ value (35.78 kcal/mol), estimated for the microenvironments inside the NPs by the use of the correlation between Φ_F of C2 and $E_T(30)$ for different solvents,[15] suggests the existence of environments able to perform polar interactions with guest molecules. This value is lower than that attributed to dichloromethane[52] but in the range of moderately polar solvents, such as 1,4-dioxane. Additionally, using the ratio of the solvent viscosity to $E_T(30)$,[15] we could estimate the microviscosity of these environments as being equal to 258.92 cP, a typical value for extremely viscous environments, capable of reducing substantially the C2 mobility. The lower Φ_F value for C2 incorporated into the NP is probably due to additional vibronic coupling, a result of the interactions between

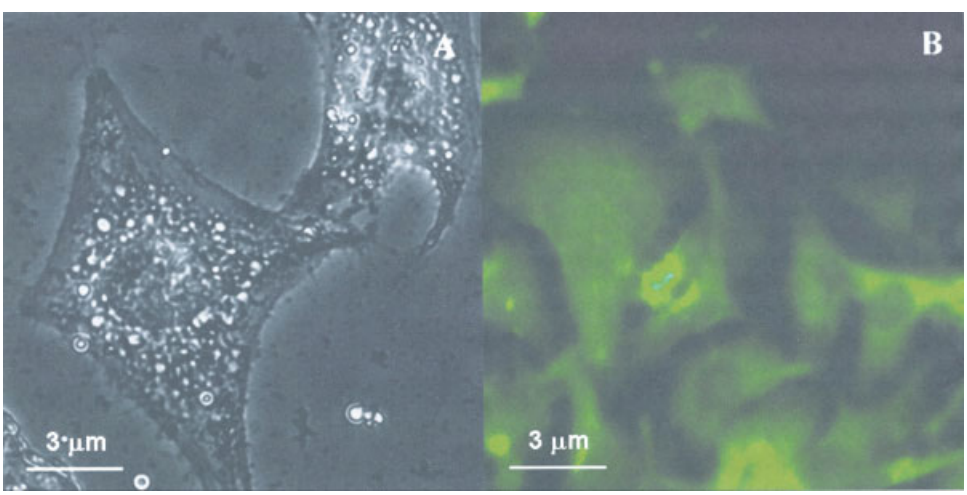

Figure 9 Cellular uptake and distribution of PLGA NPs with coumarin in B16-F10 cells incubated for 2 h: (A) phase-contrast and (B) fluorescence microscopy. The original magnification was 400×. The scale bar is equal to 3 µm. [Color figure can be viewed in the online issue, which is available at www.interscience.wiley.com.]

C2 and polar moieties associated with the structure of the NPs. In a previous work, this probe was shown to be able to estimate the microviscosity of cationic and anionic surfactants, typical models of organized systems.[15] The values found were compatible with the expected values, of we consider that for sodium dodecyl sulfate micelles, the reported value for the hydrophobic environment varies between 4 and 193 cP.[54–61]

Cytotoxicity and cellular uptake of NPs

As shown in Figure 8, the cell viability after 24 h of incubation (measured via the metabolism of MTT to a purple formazan dye by mitochondrial succinate dehydrogenase in viable cells) was not significantly reduced in cultures containing coumarin (1×10^{-6} to 1×10^{-3} mol/L). With the maximum concentration considered in these assays, the maximum reduction in the cell viability was 15.8 ± 6.7%. The cytotoxicity effect of C2 over B16-F10 murine cells also diminished when C2 was encapsulated in NPs, suggesting efficient drug entrapment.

The great advantages of C2's low toxicity and high Φ_F value make this system feasible for use as an intracellular fluorescence probe. The encapsulation method evaluated in this report for C2 loaded in PLGA has been shown to be effective, giving stable spectroscopic characteristics, good physicochemical stability, and efficient uptake by neoplasic cells, as shown in Figure 9.

CONCLUSIONS

PLGA NPs were successfully prepared with the solvent-evaporation technique. A high level of drug incorporation (up to 70%) could be reached for the incorporation of C2, a hydrophobic compound. The observed release profile is slow and self-sustained and is probably influenced by the low porosity of the NP, as observed by SEM measurements, and the hydrophobicity of the encapsulated drug. NP–C2 presented a mean diameter of 253 nm, slightly higher than that of the ENP, a low polydispersity, and a low tendency to suffer aggregation; the last was suggested by the slightly positive ζ potential. The NP–C2 FTIR spectrum does not show important changes when compared with the ENP spectrum, most likely because of the small concentration of aminocoumarin. However, DSC, spectrometric, and photophysical data have been shown to be sufficiently sensitive to reveal that C2 interacts dynamically through polar intermolecular interactions, most likely involving the diethylamino moiety and ester groups from the NPs, as suggested by the analysis of the electron density map of C2.

The use of C2 as a fluorescent probe furnished important information about the nature of the environments created during the preparation of the NPs, confirming its versatility and good sensitivity. The polarity of the microenvironments in which C2 was allocated, expressed in terms of the $E_T(30)$ scale (35.78 kcal/mol), suggests that they are moderately polar, whereas the probing of the viscosity shows that they are strongly viscous (258.92 cP), reducing substantially the mobility of the probe.

The increase in the NP mobility induced by C2 incorporation and the vibronic coupling, resulting from the intermolecular interactions between C2 and ester groups from the NPs, are not sufficient to cause a substantial decrease in the value of Φ_F of C2, preserving its photophysical properties.

The light scattering induced by the NPs in a suspension did not affect significantly the fluorescence measurements because the emission spectra were obtained with sufficiently diluted solutions and suspensions with the aim of avoiding internal filter effects, and the excitation wavelength was sufficiently shifted from the range in which strong light scattering was observed.

NP–C2 was uptaken by B16-F10 cells and shown to be nontoxic at the evaluated concentrations, and this suggests that the NP–C2 system is a promising candidate as a cytoplasmatic fluorescent probe.

References

1. Jeon, H.-J.; Jeong, Y.-I.; Jang, M.-K.; Park, Y.-H.; Nah, J.-W. Int J Pharm 2000, 207, 99.
2. Lacasse, F. X.; Fillion, M. C.; Phillips, N. C.; Escher, E.; McMullen, J. N.; Hildgen, P. Pharm Res 1998, 15, 312.
3. Okada, H.; Toguchi, H. Crit Rev Ther Drug Carrier Syst 1995, 12, 1.
4. Jain, R. A. Biomaterials 2000, 21, 2475.
5. Konan, Y. N.; Chevallier, J.; Gurny, R.; Allémann, E. Photochem Photobiol 2003, 77, 638.
6. Fu, J.; Li, X.; Ng, D. K. P.; Wu, C. Langmuir 2002, 18, 3843.
7. Kumar, M. N. V. R.; Bakowsky, U.; Lehr, C. M. Biomaterials 2004, 25, 1771.
8. Panyam, J.; Labhasetwar, V. Adv Drug Delivery Rev 2003, 55, 329.
9. Dunne, M.; Corrigan, O. I.; Ramtoola, Z. Biomaterials 2000, 21, 1659.
10. Lemoine, D.; Wauters, F.; Bouchend'homme, S.; Preat, V. Int J Pharm 1998, 176, 9.
11. Esposito, E.; Sebben, S.; Cortesi, R.; Menegatti, E.; Nastruzzi, C. Int J Pharm 1999, 189, 29.
12. Machado, A. E. H.; Severino, D.; Ribeiro, J.; De Paula, R.; Gehlen, M. H.; Oliveira, H. P. M.; Matos, M. S.; Miranda, J. A. Photochem Photobiol Sci 2004, 3, 79.
13. Machado, A. E. H.; Miranda, J. A. J Photochem Photobiol A 2001, 141, 109.
14. Machado, A. E. H.; Miranda, J. A.; Guilardi, S.; Nicodem, D. E.; Severino, D. Spectrochim Acta A 2003, 59, 345.
15. De Paula, R.; Machado, A. E. H.; Miranda, J. A. J Photochem Photobiol A 2004, 165, 109.
16. Bayrakçeken, F.; Yaman, A.; Hayvali, M. Spectrochim Acta A 2005, 61, 983.
17. Dall'Acqua, F.; Vedaldi, D.; Caffieri, S. In The Fundamental Bases of Phototherapy; Hönigsmann, H.; Jori, G.; Young, A. R., Eds.; OEMF: Milan, 1996; p 1.
18. Maeda, M. Laser Dyes; Academic: New York, 1984.

19. Christie, R. M.; Lui, H. Dyes Pigm 1999, 42, 85.
20. Chandrasekharan, N.; Kelly, L. Spectrum 2002, 15, 1.
21. Kumar, S.; Giri, R.; Mishra, S. C.; Machwe, M. K. Spectrochim Acta A 1995, 51, 1459.
22. Capek, I. Adv Colloid Interface Sci 2002, 97, 91.
23. Muthuramu, K.; Ramamurthy, V. J Photochem 1984, 26, 57.
24. Chowdhury, A.; Locknar, S. A.; Premvardhan, L. L.; Peteanu, L. A. J Phys Chem A 1999, 103, 9614.
25. Parusel, A. B. J. Chem Phys Lett 2001, 340, 531.
26. Hazra, P.; Sarkar, N. Chem Phys Lett 2001, 342, 303.
27. Arbeloa, T. L.; Arveloa, F. L.; Tapia, M. J.; Arbeloa, I. L. J Phys Chem 1993, 97, 4704.
28. Kumar, S.; Giri, R.; Mishra, S. C.; Machwe, M. K. Spectrochim Acta A 1995, 51, 1459.
29. Raju, B. B.; Varadarajan, T. S. J Phys Chem 1994, 98, 8903.
30. Gao, F.; Li, H.-R.; Yang, Y.-Y. Dyes Pigm 2000, 47, 231.
31. Luan, X. H.; Cerqueira, N. M. F. S. A.; Oliveira, A. M. A. G.; Raposo, M. M.; Rodrigues, L. M.; Coelho, P.; Campos, A. M. F. O. Adv Colour Sci Technol 2002, 5, 18.
32. Gomes, A. J.; Lunardi, L. O.; Marchetti, J. M.; Lunardi, C. N.; Tedesco, A. C. Drug Delivery 2005, 12, 159.
33. Sahoo, S. K.; Panyam, J.; Prabha, S.; Labhasetwar, V. J Controlled Release 2002, 82, 105.
34. Lunardi, C. N.; Tedesco, A. C.; Kurth, T. H.; Brinn, I. M. Photochem Photobiol Sci 2003, 2, 954.
35. Eaton, D. F. Pure Appl Chem 1988, 60, 1107.
36. Moridani, M. Y.; Moore, M.; Bartsch, R. A.; Yang, Y. F.; Heibati-Sadati, S. J Pharm Sci 2005, 8, 348.
37. Frisch, M. J.; Trucks, G. W.; Schlegel, H. B.; Scuseria, G. E.; Robb, M. A.; Cheeseman, J. R.; Montgomery, J. A., Jr.; Vreven, T.; Kudin, K. N.; Burant, J. C.; Millam, J. M.; Iyengar, S. S.; Tomasi, J.; Barone, V.; Mennucci, B.; Cossi, M.; Scalmani, G.; Rega, N.; Petersson, G. A.; Nakatsuji, H.; Hada, M.; Ehara, M.; Toyota, K.; Fukuda, R.; Hasegawa, J.; Ishida, M.; Nakajima, T.; Honda, Y.; Kitao, O.; Nakai, H.; Klene, M.; Li, X.; Knox, J. E.; Hratchian, H. P.; Cross, J. B.; Adamo, C.; Jaramillo, J.; Gomperts, R.; Stratmann, R. E.; Yazyev, O.; Austin, A. J.; Cammi, R.; Pomelli, C.; Ochterski, J. W.; Ayala, P. Y.; Morokuma, K.; Voth, G. A.; Salvador, P.; Dannenberg, J. J.; Zakrzewski, V. G.; Dapprich, S.; Daniels, A. D.; Strain, M. C.; Farkas, O.; Malick, D. K.; Rabuck, A. D.; Raghavachari, K.; Foresman, J. B.; Ortiz, J. V.; Cui, Q.; Baboul, A. G.; Clifford, S.; Cioslowski, J.; Stefanov, B. B.; Liu, G.; Liashenko, A.; Piskorz, P.; Komaromi, I.; Martin, R. L.; Fox, D. J.; Keith, T.; Al-Laham, M. A.; Peng, C. Y.; Nanayakkara, A.; Challacombe, M.; Gill, P. M. W.; Johnson, B.; Chen, W.; Wong, M. W.; Gonzalez, C.; Pople, J. A. Gaussian 03, Revision B.05; Gaussian: Pittsburgh, PA, 2003.
38. Schlicher, E. J. A. M.; Postma, N. S.; Zuidema, J.; Talsma, H.; Hennink, W. E. Int J Pharm 1997, 153, 235.
39. Kompella, U. B.; Bandi, N.; Ayalasomayajula, S. P. Drug Delivery Technol 2001, 1, 32.
40. Shaweh, M.; Besnard, M.; Nicolas, V.; Fattal, E. Eur J Pharmacol Biopharm 2005, 61, 1.
41. Zambaux, M. F.; Bonneaux, F.; Gref, R.; Maincent, P.; Dellacherie, E.; Alonso, M. J.; Labrude, P.; Vigneron, C. J Controlled Release 1998, 50, 31.
42. Gomes, A. J.; Faustino, A. S.; Lunardi, C. N.; Lunardi, L. O.; Machado, A. E. H. Int J Pharm 2007, 332, 153.
43. Gomes, A. J.; Faustino, A. S.; Machado, A. E. H.; Zaniquelli, M. E. D.; Rigoletto, T. P.; Lunardi, C. N.; Lunardi, L. O. Drug Delivery 2006, 13, 447.
44. Ruan, G.; Feng, S.-S. Biomaterials 2003, 24, 5037.
45. Castelli, F. Int J Pharm 1998, 176, 85.
46. Turro, N. J. Modern Molecular Photochemistry; University Science Books: Mill Valley; CA, 1991.
47. Gilbert, A.; Baggott, J. Essentials of Molecular Photochemistry; Blackwell: London, 1991.
48. Seixas de Melo, J.; Becker, R. S.; Maçanita, A. L. J Phys Chem 1994, 98, 6054.
49. Barik, A.; Kumbhakar, M.; Nath, S.; Pal, H. Chem Phys 2005, 315, 277.
50. Dahiya, P.; Kumbhakar, M.; Mukherjee, T.; Pal, H. Chem Phys Lett 2005, 414, 148.
51. Hazra, P.; Sarkar, N. Chem Phys Lett 2001, 342, 303.
52. Reichardt, C. Chem Rev 1994, 94, 2319.
53. Kwok, W.-M.; George, M. W.; Grills, D. C.; Ma, C.; Matousek, P.; Parker, A. W.; Phillips, D.; Toner, W. T.; Towrie, M. Angew Chem Int Ed 2003, 42, 1826.
54. Kalyanasundaram, K. Photochemistry in Microheterogeneous Systems; Academic: Orlando, FL, 1987.
55. Emert, J.; Behrens, C.; Goldenberg, M. J Am Chem Soc 1979, 101, 771.
56. Turro, N. J.; Aikawa, M.; Yekta, A. J Am Chem Soc 1979, 101, 772.
57. Turro, N. J.; Okubo, T. J Am Chem Soc 1981, 103, 7224.
58. Miller, D. J. Ber Bunsenges Phys Chem 1981, 85, 337.
59. Pownall, H. J.; Smith, L. C. J Am Chem Soc 1972, 95, 3136.
60. Thomas, J. K. Chem Rev 1980, 80, 283.
61. Zacchariasse, K. A. Chem Phys Lett 1978, 57, 429.